

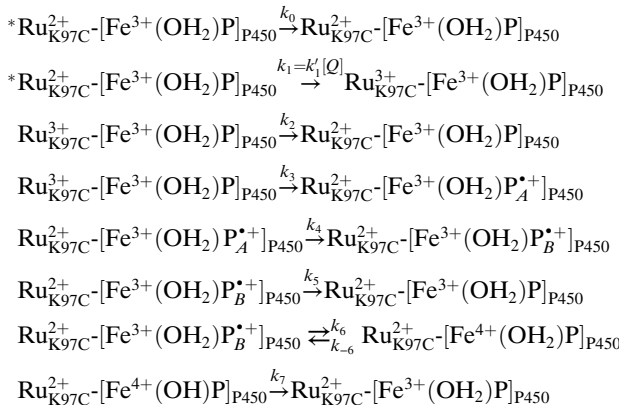
Supporting Information

Ener et al. 10.1073/pnas.1012381107

SI Text

Crystal Structure Determination. Diffraction data were processed with Mosflm (1) and Scala (2). Initial model for the Ru^{II}_{K97C}-Fe^{III}_{P450} structure was derived from the palmitic acid-bound P450-BM3 structure (Protein Data Bank ID 2UWH) (3) by molecular replacement using Molrep (4). Coot (5) and Refmac5 (6) were used for model fitting and refinement. The final models were validated using the programs Procheck (7), Sfcheck (8), and Molprobity (9). Most of the above processes were done with the graphical interface to the CCP4 program suite (10). All structural graphics were generated using the Pymol Graphics System (11).

Kinetics Data Analysis. The kinetics data were analyzed in terms of the following reaction sequence:



Chemical entities are identified with the following symbols:

$$\begin{aligned}
 A &= *\text{Ru}_{\text{K97C}}^{2+}[\text{Fe}^{3+}(\text{OH}_2)\text{P}]_{\text{P450}} \\
 B &= \text{Ru}_{\text{K97C}}^{3+}[\text{Fe}^{3+}(\text{OH}_2)\text{P}]_{\text{P450}} \\
 C &= \text{Ru}_{\text{K97C}}^{2+}[\text{Fe}^{3+}(\text{OH}_2)\text{P}_A^{\bullet+}]_{\text{P450}} \\
 D &= \text{Ru}_{\text{K97C}}^{2+}[\text{Fe}^{3+}(\text{OH}_2)\text{P}_B^{\bullet+}]_{\text{P450}} \\
 E &= \text{Ru}_{\text{K97C}}^{2+}[\text{Fe}^{4+}(\text{OH})\text{P}]_{\text{P450}} \\
 F &= \text{Ru}_{\text{K97C}}^{2+}[\text{Fe}^{3+}(\text{OH}_2)\text{P}]_{\text{P450}}
 \end{aligned}$$

The differential equations describing the reaction sequence are as follows:

$$\begin{aligned}
 \frac{dA}{dt} &= -(k_0 + k_1)A \quad \frac{dB}{dt} = k_1A - (k_2 + k_3)B \quad \frac{dC}{dt} = k_3B - k_4C \\
 \frac{dD}{dt} &= k_4C - (k_5 + k_6)D + k_{-6}E \quad \frac{dE}{dt} = k_6D - (k_{-6} + k_7)E
 \end{aligned}$$

The general solution to this set of coupled first-order differential equations is a sum of five exponential functions with empirical rate constants γ_1 , γ_2 , γ_3 , γ_4 , and γ_5 . These rate constants are obtained by solving the following secular equation:

$$\begin{vmatrix}
 \gamma - (k_0 + k_1) & 0 & 0 & 0 & 0 \\
 k_1 & \gamma - (k_2 + k_3) & 0 & 0 & 0 \\
 0 & k_3 & \gamma - k_4 & 0 & 0 \\
 0 & 0 & k_4 & \gamma - (k_5 + k_6) & k_{-6} \\
 0 & 0 & 0 & k_6 & \gamma - (k_{-6} + k_7)
 \end{vmatrix} = 0.$$

The five roots to the secular equation are

$$\begin{aligned}
 \gamma_1 &= k_0 + k_1 \quad \gamma_2 = k_2 + k_3 \quad \gamma_3 = k_4 \\
 \gamma_+ &= \frac{1}{2}(k_5 + k_6 + k_{-6} + k_7) \\
 &\quad + \frac{1}{2}\sqrt{(k_5 + k_6 + k_{-6} + k_7)^2 - 4(k_5k_{-6} + k_5k_7 + k_6k_7)} \\
 \gamma_- &= \frac{1}{2}(k_5 + k_6 + k_{-6} + k_7) \\
 &\quad - \frac{1}{2}\sqrt{(k_5 + k_6 + k_{-6} + k_7)^2 - 4(k_5k_{-6} + k_5k_7 + k_6k_7)}.
 \end{aligned}$$

The boundary conditions were taken to be

$$\begin{aligned}
 A(t=0) &= A_0; \quad B(t=0) = C(t=0) = D(t=0) = E(t=0) = 0 \\
 \lim_{t \rightarrow \infty} A(t) &= \lim_{t \rightarrow \infty} B(t) = \lim_{t \rightarrow \infty} C(t) = \lim_{t \rightarrow \infty} D(t) = \lim_{t \rightarrow \infty} E(t) = 0.
 \end{aligned}$$

The time-dependent concentrations of the five reagents are given by

$$\begin{aligned}
 A(t) &= \alpha_A e^{-\gamma_1 t} = A_0 e^{-\gamma_1 t} \\
 B(t) &= \alpha_A e^{-\gamma_1 t} + \beta_A e^{-\gamma_2 t} = \frac{k_1 A_0}{\gamma_2 - \gamma_1} (e^{-\gamma_1 t} - e^{-\gamma_2 t}) \\
 C(t) &= \alpha_C e^{-\gamma_1 t} + \beta_C e^{-\gamma_2 t} + \chi_C e^{-\gamma_3 t} \\
 &= k_1 k_3 A_0 \left[\frac{e^{-\gamma_1 t}}{(\gamma_3 - \gamma_1)(\gamma_2 - \gamma_1)} - \frac{e^{-\gamma_2 t}}{(\gamma_3 - \gamma_2)(\gamma_2 - \gamma_1)} \right. \\
 &\quad \left. + \frac{e^{-\gamma_3 t}}{(\gamma_3 - \gamma_1)(\gamma_3 - \gamma_2)} \right] \\
 D(t) &= \alpha_D e^{-\gamma_1 t} + \beta_D e^{-\gamma_2 t} + \chi_D e^{-\gamma_3 t} + \delta_D e^{-\gamma_4 t} + \zeta_D e^{-\gamma_5 t} \\
 E(t) &= \alpha_E e^{-\gamma_1 t} + \beta_E e^{-\gamma_2 t} + \chi_E e^{-\gamma_3 t} + \delta_E e^{-\gamma_4 t} + \zeta_E e^{-\gamma_5 t},
 \end{aligned}$$

where

$$\begin{aligned}
\alpha_D &= \left(\frac{k_{-6} + k_7 - \gamma_1}{\gamma_1^2 - (\gamma_+ + \gamma_-)\gamma_1 + \gamma_+\gamma_-} \right) \frac{k_1 k_3 \gamma_3 A_0}{(\gamma_3 - \gamma_1)(\gamma_2 - \gamma_1)} \\
\beta_D &= \left(\frac{k_{-6} + k_7 - \gamma_2}{\gamma_2^2 - (\gamma_+ + \gamma_-)\gamma_2 + \gamma_+\gamma_-} \right) \frac{-k_1 k_3 \gamma_3 A_0}{(\gamma_3 - \gamma_1)(\gamma_2 - \gamma_1)} \\
\chi_D &= \left(\frac{k_{-6} + k_7 - \gamma_3}{\gamma_3^2 - (\gamma_+ + \gamma_-)\gamma_3 + \gamma_+\gamma_-} \right) \frac{k_1 k_3 \gamma_3 A_0}{(\gamma_3 - \gamma_1)(\gamma_3 - \gamma_2)} \\
\delta_D &= \left(\frac{\gamma_+ - k_{-6} - k_7}{\gamma_+ - \gamma_-} \right) \left[\left(\frac{\gamma_1 - \gamma_-}{k_{-6} + k_7 - \gamma_1} \right) \alpha_D + \left(\frac{\gamma_2 - \gamma_-}{k_{-6} + k_7 - \gamma_2} \right) \beta_D \right. \\
&\quad \left. + \left(\frac{\gamma_3 - \gamma_-}{k_{-6} + k_7 - \gamma_3} \right) \chi_D \right] \\
\zeta_D &= -\alpha_D - \beta_D - \chi_D - \delta_D \quad \alpha_E = \left(\frac{k_1 k_3 k_6 \gamma_3 A_0}{k_{-6} + k_7 - \gamma_1} \right) \alpha_D \\
\beta_E &= \left(\frac{k_1 k_3 k_6 \gamma_3 A_0}{k_{-6} + k_7 - \gamma_2} \right) \beta_D \quad \chi_E = \left(\frac{k_1 k_3 k_6 \gamma_3 A_0}{k_{-6} + k_7 - \gamma_3} \right) \chi_D \\
\delta_E &= \left(\frac{k_1 k_3 k_6 \gamma_3 A_0}{k_{-6} + k_7 - \gamma_+} \right) \delta_D \quad \zeta_E = \left(\frac{k_1 k_3 k_6 \gamma_3 A_0}{k_{-6} + k_7 - \gamma_-} \right) \zeta_D
\end{aligned}$$

The transient absorption kinetics data [$\Delta\text{Abs}(\lambda, t)$] can be described by the following matrix equation:

$$\begin{aligned}
&\begin{bmatrix} \Delta\text{Abs}(\lambda_1, t_1) & \Delta\text{Abs}(\lambda_2, t_1) & \dots & \Delta\text{Abs}(\lambda_m, t_1) \\ \Delta\text{Abs}(\lambda_1, t_2) & \Delta\text{Abs}(\lambda_2, t_2) & \dots & \Delta\text{Abs}(\lambda_m, t_2) \\ \vdots & \vdots & \ddots & \vdots \\ \Delta\text{Abs}(\lambda_1, t_n) & \Delta\text{Abs}(\lambda_2, t_n) & \dots & \Delta\text{Abs}(\lambda_m, t_n) \end{bmatrix} \\
&= \begin{bmatrix} e^{-\gamma_1 t_1} & e^{-\gamma_2 t_1} & e^{-\gamma_3 t_1} & e^{-\gamma_+ t_1} & e^{-\gamma_- t_1} \\ e^{-\gamma_1 t_2} & e^{-\gamma_2 t_2} & e^{-\gamma_3 t_2} & e^{-\gamma_+ t_2} & e^{-\gamma_- t_2} \\ \vdots & \vdots & \vdots & \vdots & \vdots \\ e^{-\gamma_1 t_n} & e^{-\gamma_2 t_n} & e^{-\gamma_3 t_n} & e^{-\gamma_+ t_n} & e^{-\gamma_- t_n} \end{bmatrix} \\
&\times \begin{bmatrix} \alpha_A & \alpha_B & \alpha_C & \alpha_D & \alpha_E \\ 0 & \beta_B & \beta_C & \beta_D & \beta_E \\ 0 & 0 & \chi_C & \chi_D & \chi_E \\ 0 & 0 & 0 & \delta_D & \delta_E \\ 0 & 0 & 0 & \zeta_D & \zeta_E \end{bmatrix} \\
&\times \begin{bmatrix} \Delta\epsilon_A(\lambda_1) & \Delta\epsilon_A(\lambda_2) & \dots & \Delta\epsilon_A(\lambda_m) \\ \Delta\epsilon_B(\lambda_1) & \Delta\epsilon_B(\lambda_2) & \dots & \Delta\epsilon_B(\lambda_m) \\ \Delta\epsilon_C(\lambda_1) & \Delta\epsilon_C(\lambda_2) & \dots & \Delta\epsilon_C(\lambda_m) \\ \Delta\epsilon_D(\lambda_1) & \Delta\epsilon_D(\lambda_2) & \dots & \Delta\epsilon_D(\lambda_m) \\ \Delta\epsilon_E(\lambda_1) & \Delta\epsilon_E(\lambda_2) & \dots & \Delta\epsilon_E(\lambda_m) \end{bmatrix}.
\end{aligned}$$

The molar difference spectra for the five transient species can be determined if numerical values for the elements of the exponential coefficient matrix (i.e., $\alpha_i, \beta_i, \chi_i, \delta_i, \zeta_i; i = A, B, C, D, E$) are provided. Because there are nine elementary rate constants in the model, and only five empirical rate constants obtained by fit-

- Leslie A (2006) The integration of macromolecular diffraction data. *Acta Crystallogr, Sect D: Biol Crystallogr* 62:48–57.
- Evans PR (1993) Data reduction. *CCP4 Study Weekend Proceedings DL/SCI/R34*, pp 114–122.
- Huang W, et al. (2007) Filling a hole in cytochrome P450 BM3 improves substrate binding and catalytic efficiency. *J Mol Biol* 373:633–651.
- Vagin A, Teplyakov A (1997) MOLREP: An automated program for molecular replacement. *J Appl Crystallogr* 30:1022–1025.
- Emsley P, Cowtan K (2004) Coot: Model-building tools for molecular graphics. *Acta Crystallogr, Sect D: Biol Crystallogr* 60:2126–2132.
- Murshudov GN, Vagin AA, Dodson EJ (1997) Refinement of macromolecular structures by the maximum-likelihood method. *Acta Crystallogr, Sect D: Biol Crystallogr* 53:240–255.
- Laskowski RA, MacArthur MW, Moss DS, Thornton JM (1993) Procheck—a program to check the stereochemical quality of protein structures. *J Appl Crystallogr* 26:283–291.
- Vaguine AA, Richelle J, Wodak SJ (1999) SFCHECK: A unified set of procedures for evaluating the quality of macromolecular structure-factor data and their agreement with the atomic model. *Acta Crystallogr, Sect D: Biol Crystallogr* 55:191–205.
- Lovell SC, et al. (2003) Structure validation by C alpha geometry: phi, psi and C beta deviation. *Proteins* 50:437–450.
- Potterton E, Briggs P, Turkenburg M, Dodson EJ (2003) A graphical user interface to the CCP4 program suite. *Acta Crystallogr, Sect D: Biol Crystallogr* 59:1131–1137.
- DeLano WL (2002) The PyMOL Molecular Graphics System. Available at www.pymol.org.

ting the data, it is not possible to determine empirically all of the elementary rate constants in the kinetics model. Consequently, absolute molar difference spectra cannot be evaluated, but unscaled difference spectra for the five transient species can be determined. An optimization procedure for the four adjustable parameters in the kinetics model was used to minimize the differences among the transient spectra at the three pH values for each of the five species.

Global fitting of the transient absorption kinetics to a five-exponential function for the three different solution pH values gave the following empirical rate constants (the value of γ_1 was extracted from luminescence decay measurements):

pH 6

$$\gamma_1 = 2.5 \times 10^7 \text{ s}^{-1}; \quad \gamma_2 = 1.5 \times 10^6 \text{ s}^{-1}; \quad \gamma_3 = 2.0 \times 10^5 \text{ s}^{-1}; \\ \gamma_+ = 2.0 \times 10^4 \text{ s}^{-1}; \quad \gamma_- = 6 \times 10^1 \text{ s}^{-1};$$

pH 7

$$\gamma_1 = 2.4 \times 10^7 \text{ s}^{-1}; \quad \gamma_2 = 1.5 \times 10^6 \text{ s}^{-1}; \quad \gamma_3 = 1.5 \times 10^5 \text{ s}^{-1}; \\ \gamma_+ = 1.2 \times 10^4 \text{ s}^{-1}; \quad \gamma_- = 7 \times 10^1 \text{ s}^{-1};$$

pH 8

$$\gamma_1 = 3.0 \times 10^7 \text{ s}^{-1}; \quad \gamma_2 = 2.0 \times 10^6 \text{ s}^{-1}; \quad \gamma_3 = 1.0 \times 10^5 \text{ s}^{-1}; \\ \gamma_+ = 4.0 \times 10^3 \text{ s}^{-1}; \quad \gamma_- = 3 \times 10^1 \text{ s}^{-1}.$$

The following assumptions were invoked to generate difference spectra of the transient species:

- Values in Table 1 are an average of optimized fits for two sets of data. Error is given in parentheses.
- The value of A_0 set equal to 1 for the pH 6 data. The data at pH 7 and pH 8 were normalized to give equivalent starting concentrations.
- The value of k_1 was given by $k_1 = *phi_{ET}\gamma_1$, where the quantum yield for production of Ru^{3+} , $*phi_{ET}$, was set equal to 0.8 (0.05) for the pH 6 data. Optimization gave the values of $*phi_{ET} = 0.7$ (0.15) at pH 7, and $*phi_{ET} = 0.5$ (0.2) at pH 8.
- The value of k_3 was given by $k_3 = phi_{ET}\gamma_2$, where the yield for heme oxidation by Ru^{3+} , phi_{ET} , was set equal to 0.5 (0.25) for the pH 6 data. Optimization gave the values of $phi_{ET} = 0.5$ (0.25) at pH 7, and $phi_{ET} = 0.55$ (0.05) at pH 8.
- The position of the $\text{Fe}^{3+}(\text{OH}_2)\text{P}^{+} \rightleftharpoons \text{Fe}^{4+}(\text{OH})\text{P}$ equilibrium is determined by the constant $K_{eq} = k_6/k_{-6}$. The values of K_{eq} obtained by optimization are 0.59, pH 6; 0.93, pH 7; and 10.3, pH 8.
- The rate constants for the two ground-state repopulation pathways from oxidized heme (k_5, k_7) were assumed to be equal.

The optimized difference spectra for the five transient species are shown in Fig. S5. Elementary rate constants are set out in Table S2.

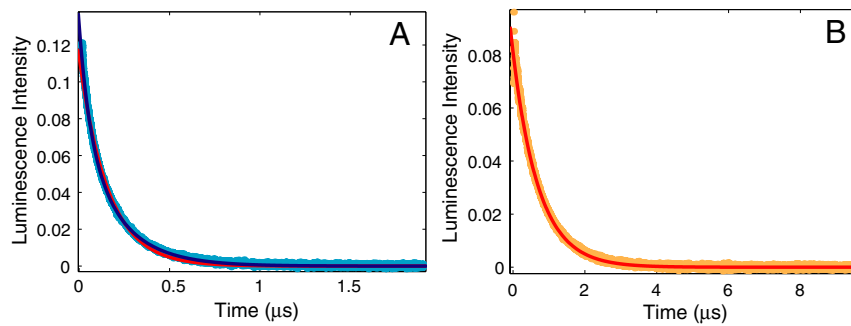


Fig. S1. ${}^*\text{Ru}^{II}\text{K97C-Fe}^{III}\text{P}_{450}$ (A) and ${}^*[\text{Ru}(\text{bpy})_2(\text{IA-phen})]^{2+}$ (B) luminescence decays at 630 nm. Monoexponential fits are in red; the biexponential fit for ${}^*\text{Ru}^{II}\text{K97C-Fe}^{III}\text{P}_{450}$ is blue.

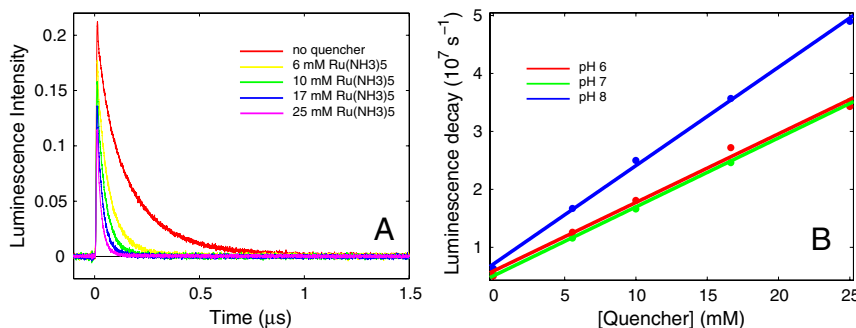


Fig. S2. $\text{Ru}(\text{NH}_3)_6^{3+}$ quenching of ${}^*\text{Ru}^{II}\text{K97C-Fe}^{III}\text{P}_{450}$ (A) Luminescence decays at 630 nm. (B) Stern–Volmer plot.

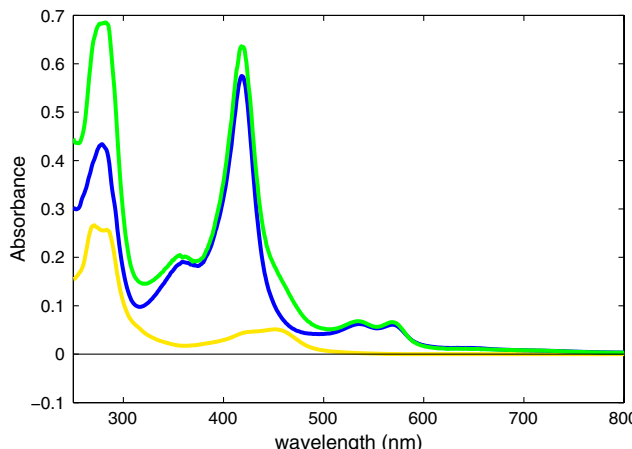


Fig. S3. UV-visible of ground/resting state species at approximately equal concentrations (yellow, ${}^*[\text{Ru}(\text{bpy})_2(\text{IA-phen})]^{2+}$; blue, BM3 K97C; green, ${}^*\text{Ru}^{II}\text{K97C-Fe}^{III}\text{P}_{450}$).

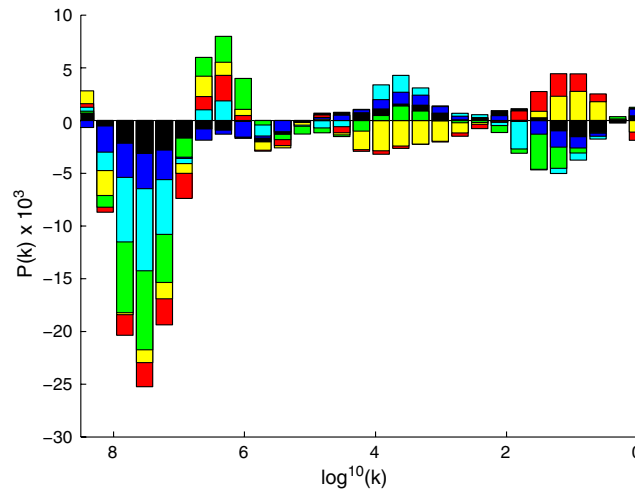


Fig. S4. Generalized singular value decomposition indicates five phases (black, 390 nm; blue, 400 nm; cyan, 410 nm; green, 420 nm; yellow, 430 nm; red, 440 nm).

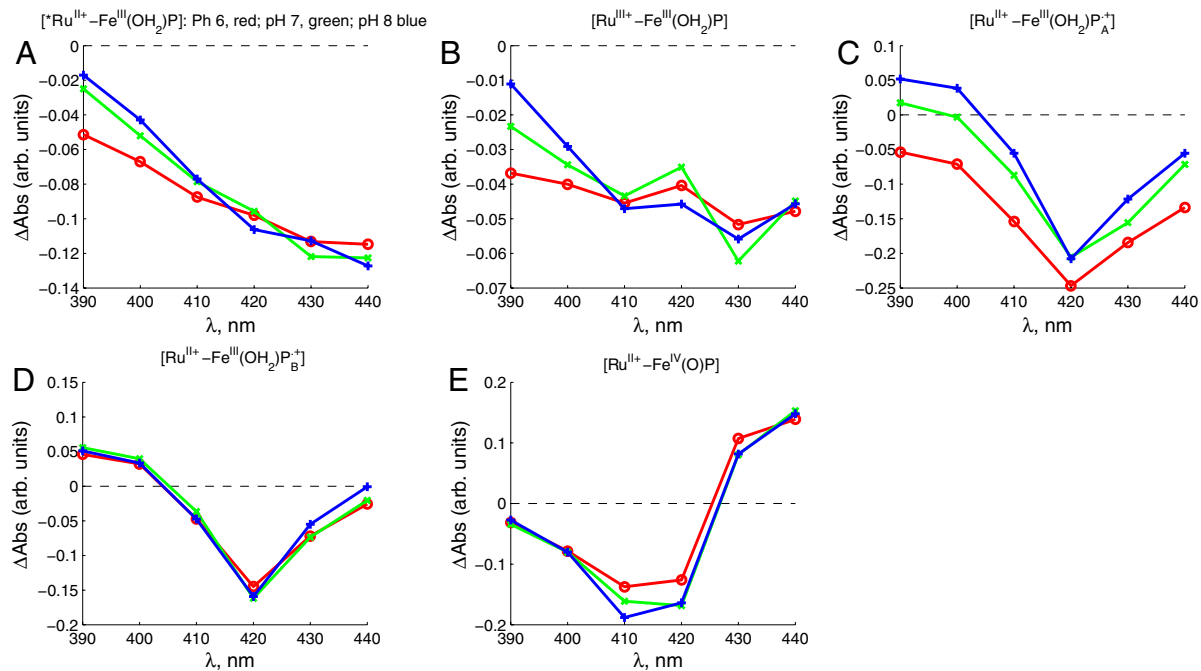


Fig. S5. Optimized difference spectra for the five transient species generated in the photochemical oxidation of $\text{Ru}^{II}_{K97C}\text{-Fe}^{III}_{P450}$ at pH 6 (red), 7 (green), and 8 (blue).

Table S1. Data collection, refinement statistics, and validation

Data collection

Wavelength, Å	0.979
Unit cell, Å	117.08, 117.08, 273.85
Space group	P41212
Resolution range, Å	45.52–2.40 (2.53–2.40)*
No. of total reflections	793,591
No. of unique reflections	74,965
Completeness, %	99.7 (99.6)
R_{merge} , %	12.6 (82.7)
$\langle I/\sigma(I) \rangle$	15.4 (4.2)
Wilson B-value, Å ²	45.6
Refinement statistics	
Resolution range, Å	10–2.4
No. of reflections used	69,343
Free R reflections, %	5.0
R/R_{free}	0.200/0.237
rmsd bond length, Å	0.0113
rmsd bond angle, deg	1.374
Ramachandran analysis, %	
No. of residues in	
Favored regions	97.4
Allowed regions	2.6
Outlier regions	0.0
PDB entry	3NPL

*Data for the outermost shell are given in parentheses.

Table S2. Elementary rate constants extracted from fitting

pH	k_0	k_1	k_2	k_3	k_4	k_5	k_6	k_{-6}	k_7	K_{eq}	${}^*\phi_{\text{ET}}$	ϕ_{ET}
6	5×10^6 (0.3×10^6)	2×10^7 (0.3×10^7)	1×10^6 (0.4×10^6)	4×10^5 (0.8×10^5)	2×10^5 (0.2×10^5)	7×10^1 (1.6×10^1)	1×10^4 (0.5×10^4)	1.5×10^4 (0.7×10^4)	7×10^1 (1.6×10^1)	0.7	0.8 (0.05)	0.5 (0.25)
7	5.5×10^6 (0.3×10^6)	1.5×10^7 (0.3×10^7)	1×10^6 (0.6×10^6)	5.5×10^5 (0.3×10^5)	1.5×10^5 (0.1×10^5)	8×10^1 (0.3×10^1)	7×10^3 (3×10^3)	4.5×10^3 (1×10^3)	8×10^1 (0.3×10^1)	1.5	0.7 (0.15)	0.5 (0.2)
8	6×10^6 (0.3×10^6)	1.5×10^7 (0.6×10^7)	1×10^6 (0.6×10^6)	8.5×10^5 (2×10^5)	1×10^5 (0.2×10^5)	4×10^1 (0.3×10^1)	3.5×10^3 (0.7×10^3)	3.5×10^2 (0.8×10^2)	4×10^1 (0.3×10^1)	10	0.5 (0.25)	0.5 (0.05)